JOURNAL OF CATALYSIS 40, 19–33 (1975)

The Catalytic Oxidation of Propylene

V. X-Ray Characterization of Iron-Containing Bismuth Molybdate Catalysts

MARIANO LOJACONO,[1] THOMAS NOTERMANN AND GEORGE W. KEULKS[2]

Department of Chemistry and Laboratory for Surface Studies, University of Wisconsin—Milwaukee, Milwaukee, Wisconsin 53201

Received March 19, 1975

The effects on phase composition and structure of adding iron to bismuth molybdate catalysts were investigated by X-ray diffraction methods. Structural and phase transformations were observed to be functions of the calcination temperature and composition. In addition, ternary compounds containing bismuth, molybdenum, and iron were identified. These ternary compounds were formed when the calcination temperature was greater than 550°C and were characterized by a monoclinic unit cell which was derived from and closely related to a scheelite unit cell. At calcination temperatures of 450°C or less, a poorly crystallized compound with a scheelite structure was identified.

INTRODUCTION

In an earlier publication, Daniel and Keulks (*1*) reported that oxide catalysts containing bismuth, iron, and molybdenum exhibited activity and selectivity comparable to bismuth molybdate for the partial oxidation of propylene to acrolein. Furthermore, they suggested that the ternary combination of Bi–Fe–Mo resulted in the formation of a distinct chemical compound which possibly was responsible for the catalytic activity and selectivity.

In contrast, Annenkova *et al.* (*2*) have reported that catalysts containing the ternary combination Bi–Fe–Mo were heterogeneous mixtures consisting of $Bi_2(MoO_4)_3$, $Fe_2(MoO_4)_3$, and oxides of bismuth with iron ($BiFeO_3$ or $Bi_2Fe_4O_9$). They concluded that the ratios of these compounds were governed by the overall chemical composition of the catalysts.

Batist *et al.* (*3*) have also examined the effect of Fe on bismuth molybdate catalysts. The catalytic properties of the system were studied over the compositional range from $Bi_2(MoO_4)_3$ to $Fe_2(MoO_4)_3$, i.e., from the α-phase of bismuth molybdate to ferric molybdate. The X-ray patterns within this range were complex, but were resolved by assuming the presence of $Bi_2(MoO_4)_3$, $Fe_2(MoO_4)_3$, Bi_2MoO_6, and a new compound, which they described as "compound X," existing over the range of Bi/Fe = 8:2 to 1:9. This compound X had never been observed in their earlier studies with Bi–Mo oxide samples, but exhibited an X-ray pattern similar to that reported by McClellan (*4*) in the patent literature for a bismuth molybdate catalyst supported on silica. This unknown compound was also an active and selective catalyst for the oxidative dehydrogenation of 1-butene to butadiene.

The combination of these experimental findings indicated that the addition of Fe to bismuth molybdate produced promising

[1] On leave of absence from Centro di Studio del C.N.R., Italy. Present address: Institute of General Chemistry, University of Rome, Rome, Italy.

[2] To whom correspondence should be addressed.

catalysts. We considered that the possible existence of new compounds within the bismuth–iron–molybdate system presents interesting structural possibilities and potentially important catalytic implications. We have, therefore, undertaken an investigation of this system with the purpose of examining the various phases present and elucidating the composition and structure of new compounds by X-ray methods.

EXPERIMENTAL METHODS

Catalyst preparation. All of the chemicals used in the preparation of the catalysts were of analytical grade. Since we had found that the α-phase of bismuth molybdate preferentially reacted with iron to form the active catalysts, we decided to standardize our preparative procedures by choosing as the first step the formation of a bismuth molybdate precipitate by a coprecipitation method which has been found to favor the formation of the α-phase of bismuth molybdate. An extensive study of this coprecipitation method has been reported earlier (*5*). The bismuth molybdate precipitate was then reacted with iron(III) hydroxide prepared from $Fe(NO_3)_3 \cdot 9H_2O$ by precipitation with dilute NH_4OH.

The two precipitates were combined and allowed to undergo a slurry reaction as described by Batist *et al.* (*6*). Specifically, this method involved removal of the mother liquor from the precipitates, combining the precipitates in 500 ml of aqueous solution of pH 4–6, stirring and heating the mixture at 70°C for 5–7 hr (until dry), grinding the resultant solid mass, and then drying at 110°C for 2 hr. The final step was calcination of the catalysts in a muffel furnace at atmospheric pressure and under ambient conditions.

The surface areas of the catalysts prepared in this study were determined by the BET method using N_2 as the adsorbate. A summary of the catalyst preparation parameters and surface areas is presented in Table 1.

TABLE 1
CATALYST PREPARATION VARIABLES AND SURFACE AREA

Sample	Atomic ratio Bi:Fe:Mo	Calcination conditions[a]	Surface area[b] (m^2/g)
1	1:0.5:1.5	M	—
2	1:1.0:1.5	M	—
3a	1:2.3:1.5	L	16.0
3b	1:2.3:1.5	H	7.2
4	1:4.0:1.5	M	11.4
5a	1:4.2:1.5	L	11.5
5b	1:4.2:1.5	H	5.6
5c	1:4.2:1.5	Y	—
5d	1:4.2:1.5	Z	—
6a	1:3.3:1	L	6.7
6b	1:3.3:1	H	3.5
6c	1:3.3:1	Z	—
7	0.6:1.4:3	H	—
8	0.6:1.4:2	H	—
9	0.6:1.4:1	H	1.8
10a	1:1:3	L	—
10b	1:1:3	H	—
11a	1:1:2	L	1.1
11b	1:1:2	H	—
12a	1:1:1	L	5.2
12b	1:1:1	H	3.5
12c	1:1:1	Z	—
13	1:1:0	H	—
14	3:1:2	H	1.0

[a] Notations L, M, H, Y, and Z indicate calcination at 450°C for 20 hr, 550°C for 20 hr, 600°C for 6 hr, 700°C for 6 hr, 700°C for 20 hr, respectively.

[b] The surface area was determined to be less than 1 m^2/g as denoted by —.

X-Ray analysis. The instrument used in this study was the Siemens COMPAK-2 X-ray diffractometer equipped with a scintillation counter. A chromium target was used in the X-ray generator because the longer wavelength of the Cr$K\alpha$ radiation ($\lambda = 2.2909$ Å) makes chromium particularly suitable for resolving lines in more complicated diffraction patterns. The Cr$K\alpha$ radiation also has an advantage over Cu$K\alpha$ radiation in that Cr$K\alpha$ radiation can be used with samples containing a large quantity of iron.

Before analyzing a sample, the diffractometer system was carefully aligned and optimized to give the most stable signal

TABLE 2
RESULTS OF ELEMENTAL ANALYSIS

Sample	Wt %			Mole ratio		
	Bi	Fe	Mo	Bi	Fe	Mo
12	44.3	12.6	25.8	0.97	1.00	1.19
14	57.4	6.95	19.4	3.00	1.31	2.15

and the highest signal-to-noise ratio. These adjustments were done with a gold sample, utilizing the Au (111) reflection. By this procedure, it was possible to determine the 2θ value of the Au (111) reflection at 58.20° (20°C) with an accuracy of ±0.02°.

Elemental analysis. The quantity of molybdenum present was determined by neutron activation analysis, and the quantities of Bi and Fe present were determined by atomic absorption spectroscopy. Repetition of the experiments showed a variation of ±10% in the absolute weight of the metals, however, the mole ratios appeared to be constant within ±2%. The calculated ratios, appearing in Table 2 for samples 12 and 14, are believed to be accurate to ±2% relative, but the absolute weight percent is only accurate to ±10% relative.

RESULTS

The catalyst preparations reported in this study were designed to examine the effects on structure and phase composition produced by varying the calcination temperature and the Bi/Fe/Mo atomic ratio. The Bi/Fe/Mo ratios were selected so as to examine the effects produced by (a) increasing the Fe content while maintaining a Bi/Mo ratio of 2:3 (samples 1–5), and (b) decreasing the Mo content while maintaining a Bi/Fe ratio of 3:7 (samples 7–9) or decreasing the Mo content while maintaining a Bi/Fe ratio of 1:1 (samples 10–13). Two additional catalysts (samples 6 and 14) were examined but have compositions other than those described above (see Table 1).

X-Ray results for catalysts of group 1 along with those for catalyst 6 are presented in Figs. 1–3. The X-ray results for catalysts of group 2 together with those for catalyst 14 are presented in Figs. 4–6. The interpretation of the X-ray data is based upon the published patterns of Aykan (*7*), Fagherazzi and Pernicone (*8*), Aravindakshan and Ali (*9*), Zaslavskii and Tutov (*10*), McClellan (*4*), and Batist *et al.* (*3*), respectively, as follows:

α-Bismuth Molybdate, $Bi_2(MoO_4)_3$

d = 7.89, 6.97, 6.29, 4.90, 4.57, 3.62, 3.59, 3.34, 3.27, 3.19, 3.05 (most characteristic), 2.88, 2.80, 2.49, 2.25, 2.00, 1.92, 1.88, 1.80, 1.76, 1.72, 1.70, 1.59.

Ferric Molybdate, $Fe_2(MoO_4)_3$

d = 6.42, 5.79, 4.55, 4.35, 4.10, 3.885, 3.576, 3.469, 3.252, 2.965, 2.899, 2.851, 2.640.

α-Fe_2O_3

d = 3.66, 2.69, 2.51, 2.20, 1.84, 1.69, 1.60, 1.48, 1.45, 1.35, 1.31, 1.26, 1.21, 1.19.

$BiFeO_3$

d = 3.95, 2.81, 2.79, 2.31, 2.28, 1.98, 1.78, 1.76, 1.63, 1.62, 1.61, 1.41, 1.40, 1.33, 1.32, 1.31, 1.26, 1.25, 1.20, 1.19.

Poorly Crystallized Compound

d = 4.86, 3.14, 2.93, 2.63, 2.31, 1.95, 1.86, 1.73, 1.60, 1.57, 1.28, 1.27.

Compound X

d = 4.88, 4.79, 3.17, 3.14, 2.90, 2.69, 2.63, 2.49, 2.32, 1.95, 1.89, 1.87, 1.73, 1.60, 1.57, 1.28, 1.27.

The X-ray patterns of the samples were also compared with the published patterns of Bi_2MoO_6 (*11*), $Bi_2Mo_2O_9$ (*12*), Bi_2O_3 (*13*), and MoO_3 (*14*). A summary of the interpretation of the X-ray data is presented in Table 3.

Several noteworthy features are appar-

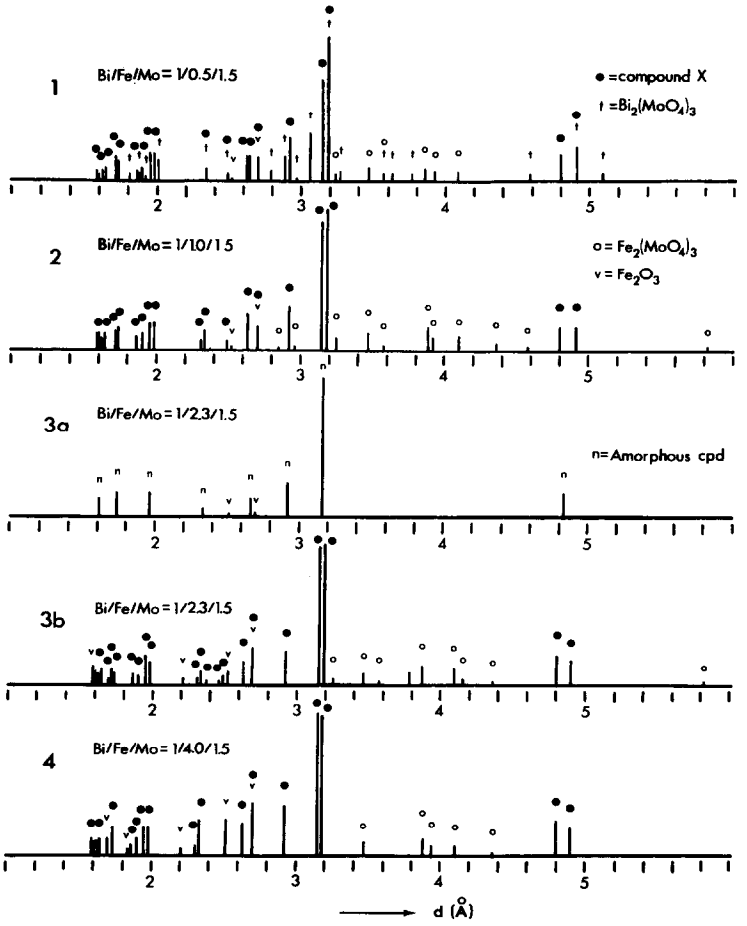

FIG. 1. X-Ray data for group 1 catalysts.

ent if one examines the X-ray results for catalysts 1–5 which represent the group 1 catalysts. The X-ray pattern of catalyst 1, with the atomic ratio of Bi/Fe/Mo = 1:0.5:1.5, reveals that the material is a mixture containing the α-phase of bismuth molybdate and compound X. There also is evidence for the presence of a small amount of $Fe_2(MoO_4)_3$ (lines at $d = 4.10$, 3.93, 3.88, 3.47, 3.25) and a trace of α-Fe_2O_3 (lines at $d = 2.69$ and 2.52). With an increase in the Fe content, catalyst 2, we observe a fundamental difference in the X-ray pattern: the α-phase of bismuth molybdate is no longer detected, but the intensities of the lines characteristic for $Fe_2(MoO_4)_3$ and compound X increase. Thus, we conclude that this preparation yields a mixture of compound X with an appreciable amount of $Fe_2(MoO_4)_3$ and also a trace of α-Fe_2O_3.

If we examine the X-ray patterns of catalysts 3a and 3b which have the same atomic ratio of Bi/Fe/Mo = 1:2.3:1.5, but calcined, respectively, at 450 and 600°C, we find that catalyst 3a contains primarily the poorly crystallized compound, i.e., the X-ray diffraction lines are substantially reduced in intensity and remain as broad diffuse bands, together with what appears to be the incipient nucleation of α-Fe_2O_3 (lines at $d = 2.69$ and 2.51 are barely de-

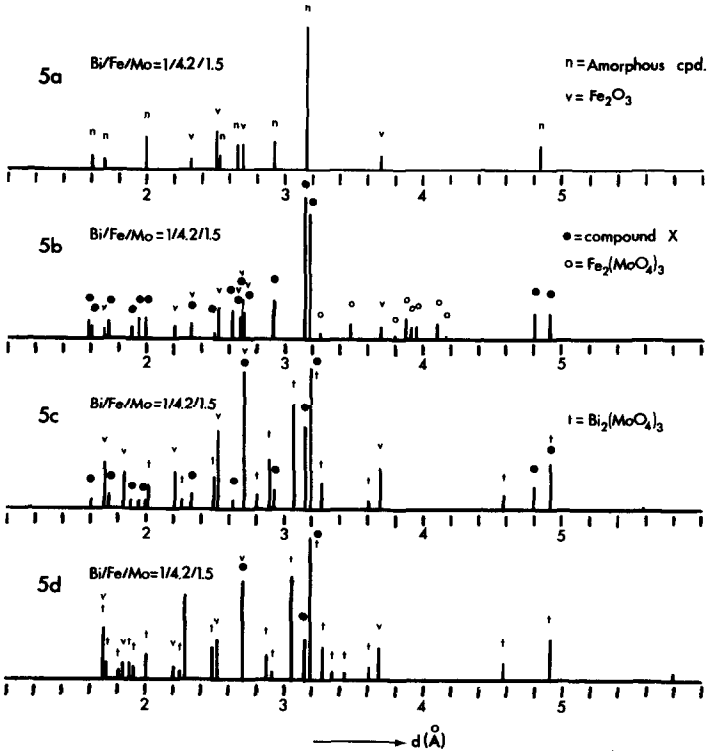

FIG. 2. X-Ray data for group 1 catalysts.

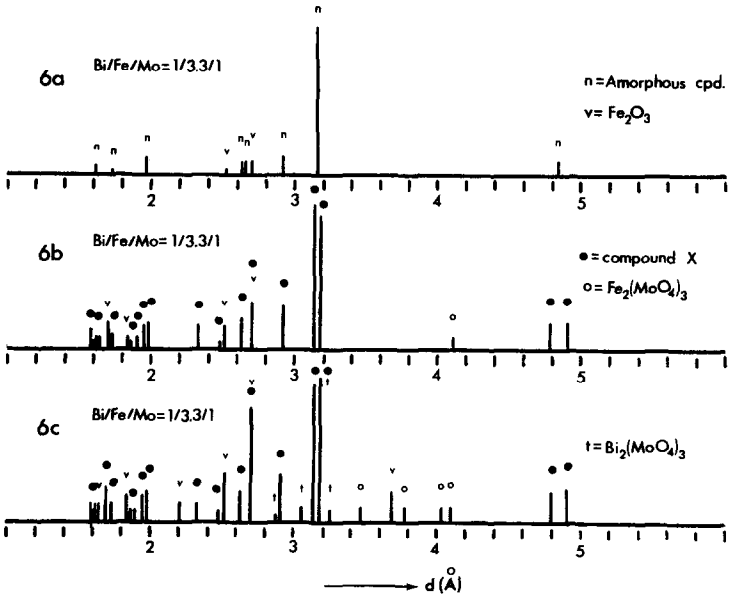

FIG. 3. X-Ray data for sample 6.

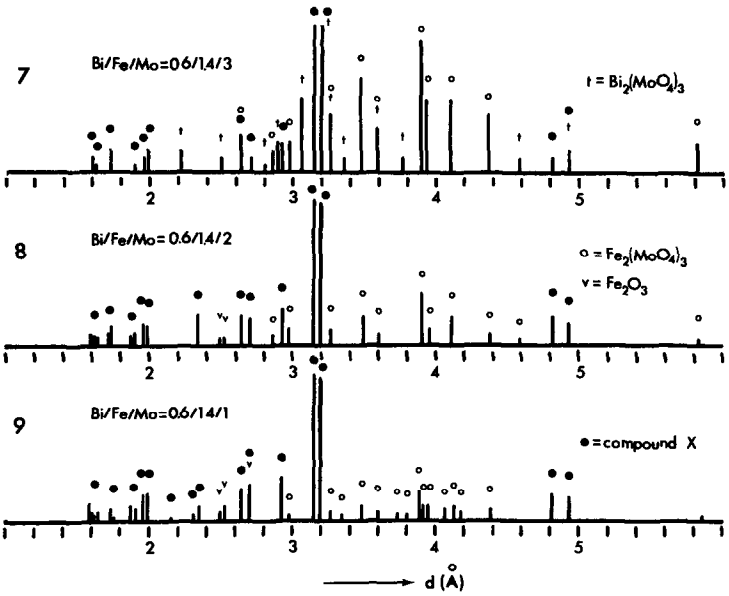

FIG. 4. X-Ray data for group 2 catalysts.

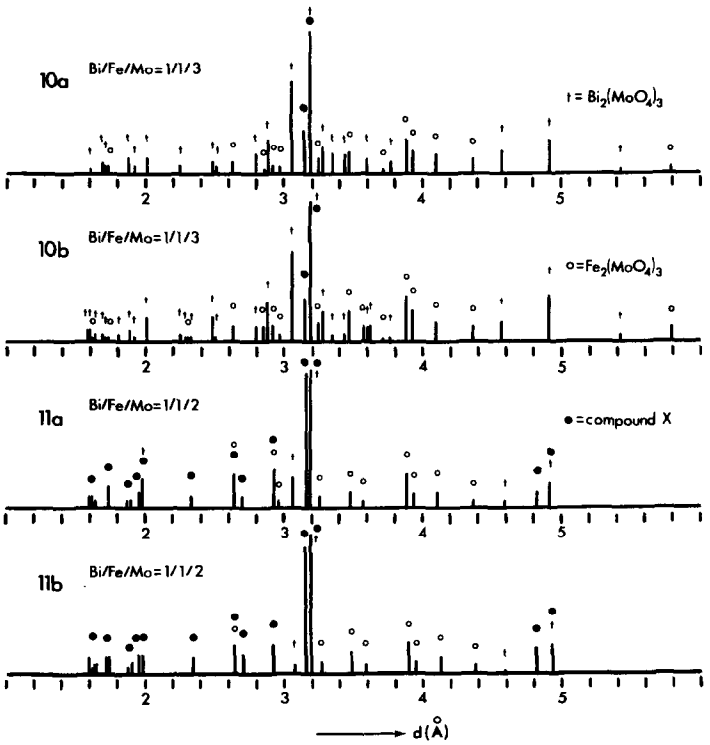

FIG. 5. X-Ray data for group 2 catalysts.

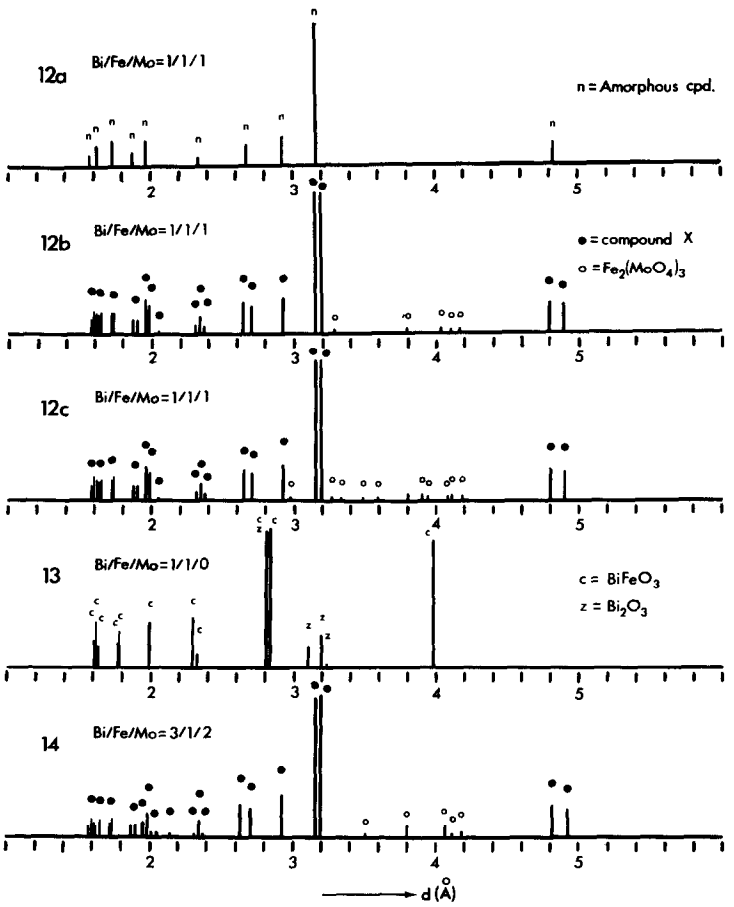

FIG. 6. X-Ray data for group 2 catalysts and catalyst 14.

tectable). On the other hand, the pattern for catalyst 3b, calcined at 600°C, shows that the material is now well crystallized and contains predominantly compound X and α-Fe_2O_3, along with an appreciable amount of $Fe_2(MoO_4)_3$.

Increasing the Fe content further, catalyst 4, we find produces a mixture now of compound X and α-Fe_2O_3, along with a small amount of $Fe_2(MoO_4)_3$. The series of catalysts represented by 5a, 5b, 5c, and 5d in Fig. 2 correspond to catalysts prepared with the atomic ratio of Bi/Fe/Mo = 1:4.2:1.5, but calcined at 450, 600 and 700°C for 6 hr, and 700°C for 24 hr, respectively. The X-ray pattern of 5a indicates the presence of the poorly crystallized compound with a small amount of α-Fe_2O_3 also being detected. Increasing the calcination temperature to 600°C, catalyst 5b, produces an increase in crystallinity, a transformation of the poorly crystallized compound into compound X, and a massive segregation of α-Fe_2O_3, as revealed by the X-ray pattern. A very small amount of ferric molybdate also was detected. The X-ray patterns for catalysts 5c and 5d, which were calcined at 700°C, indicate a large decrease in the intensities of the lines associated with compound X. At the same time, the diffraction lines characteristic of α-bismuth molybdate appear, and their intensities increase with time of calcination at 700°C, i.e., from 5c

TABLE 3
SUMMARY OF X-RAY DATA INTERPRETATION

Sample	Principal phases	Minor phases	Trace phases
1	$Bi_2(MoO_4)_3$, compound X	$Fe_2(MoO_4)_3$	Fe_2O_3
2	Compound X, $Fe_2(MoO_4)_3$		Fe_2O_3
3a	Poorly crystallized compound		Fe_2O_3
3b	Compound X, Fe_2O_3	$Fe_2(MoO_4)_3$	
4	Compound X, Fe_2O_3	$Fe_2(MoO_4)_3$	
5a	Poorly crystallized compound	Fe_2O_3	
5b	Compound X, Fe_2O_3	$Fe_2(MoO_4)_3$	
5c	Fe_2O_3, $Bi_2(MoO_4)_3$	Compound X	
5d	Fe_2O_3, $Bi_2(MoO_4)_3$	Compound X	
6a	Poorly crystallized compound		Fe_2O_3
6b	Compound X, Fe_2O_3	$Fe_2(MoO_4)_3$	
6c	Compound X, Fe_2O_3	$Bi_2(MoO_4)_3$	
7	Compound X, Fe_2 $Fe_2(MoO_4)_3$	$Bi_2(MoO_4)_3$	
8	Compound X	$Fe_2(MoO_4)_3$	
9	Compound X	$Fe_2(MoO_4)_3$	Fe_2O_3
10a	$Bi_2(MoO_4)_3$, $Fe_2(MoO_4)_3$	Compound X	
10b	$Bi_2(MoO_4)_3$, $Fe_2(MoO_4)_3$	Compound X	
11a	Compound X	$Fe_2(MoO_4)_3$	$Bi_2(MoO_4)_3$
11b	Compound X	$Fe_2(MoO_4)_3$	$Bi_2(MoO_4)_3$
12a	Poorly crystallized compound		
12b	Compound X		$Fe_2(MoO_4)_3$
12c	Compound X		$Fe_2(MoO_4)_3$
13	$BiFeO_3$	Bi_2O_3	
14	Compound X		$Fe_2(MoO_4)_3$

to 5d. Furthermore, the ferric molybdate present in 5b is no longer detected, and the α-Fe_2O_3 remains and becomes more crystalline with increasing time of calcination.

Catalysts 6a, 6b and 6c have the same atomic ratio Bi/Fe/Mo = 1:3.3:1 but have been calcined at 450, 600 and 700°C, respectively. The X-ray pattern of 6a was quite similar to that of 5a and indicated the presence of the poorly crystallized compound with a trace of Fe_2O_3. With an increase in the calcination temperature of the catalysts, the X-ray pattern of 6b reveals an increase in crystallinity, the transformation of the poorly crystallized compound into compound X, and a massive segregation of α-Fe_2O_3. The major difference between 6b and 6c is that the X-ray pattern for 6b reveals a small amount of ferric molybdate to be present, whereas the X-ray pattern for 6c, calcined at 700°C, indicates that ferric molybdate is no longer present, and a small amount of $Bi_2(MoO_4)_3$ appears instead. Annenkova *et al.* (*2*) also observed the instability of $Fe_2(MoO_4)_3$ and the formation of $Bi_2(MoO_4)_3$ in their ternary oxide mixture above 600°C. In contrast to the previous results of the group 1 catalysts 5c and 5d where compound X is unstable at 700°C, compound X remains stable in catalyst 6c at 700°C.

Consideration of the previous results for the group 1 catalysts and for catalysts 6a, 6b and 6c led to the preparation of catalysts of group 2 aimed at examining the effect of decreasing the Mo content while maintaining a constant Bi/Fe atomic ratio, i.e., decreasing the amount of Mo available to form bismuth molybdate and ferric molybdate. The amount of Fe was chosen so as not to cause massive segregation of α-Fe_2O_3.

The X-ray data for the catalysts 7, 8,

and 9 of group 2 with the same Bi/Fe ratio of 3:7 but with decreasing amounts of molybdenum, respectively, reveals further information concerning the composition of compound X. The X-ray pattern of catalyst 7 with the atomic ratio Bi/Fe/Mo = 0.6:1.4:3 indicates the presence of compound X and $Fe_2(MoO_4)_3$. The α-phase of bismuth molybdate is also present as a minor constituent of this mixture. With a decrease in the molybdenum content, catalyst 8, several important changes in the phase composition are detected in the X-ray pattern. The α-phase of bismuth molybdate is no longer observed, the characteristic intensities of $Fe_2(MoO_4)_3$ decrease, and the characteristic intensities of compound X increase. Further decrease in the molybdenum content, catalyst 9, has the effect of increasing the amount of compound X and decreasing the amount of $Fe_2(MoO_4)_3$. The X-ray pattern of this catalyst reveals that a small amount of α-Fe_2O_3 is also present.

The remaining catalysts of group 2, samples 10, 11, 12 and 13, have the same Bi/Fe ratio of 1:1, but again with decreasing amounts of molybdenum, respectively. When the Bi/Fe/Mo atomic ratio is maintained at 1:1:3, catalysts 10a and 10b, the X-ray patterns indicate the presence of the α-phase of bismuth molybdate and $Fe_2(MoO_4)_3$. A small amount of compound X is detected, but in contrast to the results discussed earlier, the only effect of the calcination temperature is to increase the degree of crystallinity. There was no evidence for the formation of a poorly crystallized compound at a calcination temperature of 450°C. In fact, the mixture maintained its compositional integrity even at a calcination temperature of 700°C. Decreasing the amount of molybdenum, catalysts 11a and 11b, results in a decrease in $Fe_2(MoO_4)_3$ and a considerable decrease in the characteristic intensities of the α-phase of bismuth molybdate. The characteristic intensities of compound X increase for both 11a and 11b; however, there is again no evidence for the formation of a poorly crystallized compound at the 450°C calcination temperature.

If we examine the X-ray patterns of catalysts 12a, 12b and 12c, we find that catalyst 12a, calcined at 450°C, exhibits the typical pattern of the poorly crystallized compound while an increase in the calcination temperature, catalyst 12b, results in the transformation of the poorly crystallized compound into compound X. The X-ray pattern of catalyst 12b provides evidence that this substance is compound X with less than 5% of $Fe_2(MoO_4)_3$ present as an impurity. An examination of this

TABLE 4
X-RAY DATA FOR THE POORLY CRYSTALLIZED COMPOUND

hkl	d_{calc}[a]	*I*	d_{obs}[b]	I/I_0	d_{obs}[c]	I/I_0
101	4.80	m	4.86	3	4.83	16
112	3.14	vvs	3.14	100	3.16	100
004	2.925	m	2.93	18	2.92	20
200	2.630	m	2.63	17	2.66	15
202	2.399	vvw				
211	2.306	w	2.31	4	2.33	6
114	2.299	vw				
105	2.138	vw				
213	2.014	vw				
204	1.956	ms	1.95	20	1.96	18
220	1.860	mw	1.86	8	1.87	10
116	1.727	m	1.73	11	1.726	18
215	1.659	vw				
303–312	1.600	m	1.60	15	1.616	15
206–224	1.566–1.569	mw	1.57	7	1.570	8
321	1.447	vvw				
008	1.462	vvw				
305	1.403	vvw				
323	1.366	vvw				
217	1.362	vvw				
400	1.315	vvw				
208	1.278	w	1.28	3	1.286	4
411	1.268	vvw				
316	1.266	w	1.27	5	1.269	4
332	1.213	vw				
404	1.199	vw				

[a] d_{calc}, based on tetragonal lattice parameters, a = 5.26 Å, c = 11.70 Å. Intensity notations s, m, and w indicate strong, medium, and weak, respectively.

[b] Lattice spacings reported by McClellan (*4*).

[c] Lattice spacings observed for sample 12a.

substance calcined at 700°C, catalyst 12c, reveals that compound X maintains its stability even at this temperature. In Table 4, the observed lattice spacings d_{hkl} for the poorly crystallized compound are compared with the calculated lattice spacings d_{hkl} for a tetragonal lattice. A comparison of the observed lattice spacings d_{hkl} for compound X with the calculated lattice spacings for a monoclinic cell is presented in Table 5.

The final catalyst preparation in group 2, catalyst 13, contains no molybdenum, and the X-ray results show that it consists of $BiFeO_3$ with a minor amount of Bi_2O_3.

Considerations concerning the composition and structure of compound X which are presented in the Discussion led to the preparation of catalyst 14 with a composition other than that of the group 1 or group 2 catalysts (see Table 1). The X-ray pattern shows that this substance is primarily one compound together with only a trace amount of $Fe_2(MoO_4)_3$ present as an impurity. The lattice spacings d_{hkl} observed for this compound are similar to those observed for compound X (sample 12b), but the intensities associated with the lattice spacings differ for the two compounds (Table 5).

TABLE 5
X-RAY DATA FOR COMPOUND X

hkl	d_{calc}[a]	I	d_{obs}[b]	I/I_0	d_{obs}[c]	I/I_0
110	4.90	m	4.90	20	4.92	20
011	4.81	m	4.80	21	4.81	23
$\bar{1}21$	3.19	vvs	3.19	100	3.19	100
130	3.16	mw				
121	3.15	vvs	3.15	100	3.15	98
031	3.14	mw				
040	2.925	m	2.924	25	2.924	30
200	2.699	mw	2.700	19	2.701	20
002	2.645	m	2.637	22	2.632	23
220	2.451	vvw				
$\bar{2}11$	2.371	mw	2.369	5	2.367	2
$\bar{1}12$	2.343	mw	2.337	12	2.335	12
211	2.340	mw				
112	2.312	mw	2.309	6	2.312	2
$\bar{1}41$	2.320	vvw				
141	2.305	vvw				
150	2.147	vvw				
051	2.140	vvw			2.139	2
$\bar{2}31$	2.057	vvw	2.054	1	2.052	3
231	2.036	vvw				
132	2.018	vvw				
$\bar{1}32$	2.038	vvw			2.008	3
240	1.984	m	1.982	20	1.982	17
042	1.962	m	1.955	24	1.952	11
$\bar{2}02$	1.9058	w	1.900	10	1.901	8
202	1.8729	w	1.867	10	1.867	8
$\bar{1}61$	1.7360	m	1.733	15	1.732	12
161	1.7296	m	1.724	15	1.725	10
$\bar{3}21$	1.6439	mw	1.640	15	1.647	12
330	1.6341	mw				
321	1.6279	mw	1.625	13	1.625	7
$\bar{1}23$	1.6189	mw				
033	1.6065	mw	1.609	14	1.609	10
123	1.6035	mw				
$\bar{2}42$	1.5968	mw	1.592	16	1.592	12
260	1.5807	mw				
242	1.5773	mw	1.571	10	1.571	8
062	1.5695	mw				

[a] d_{calc}, based on monoclinic lattice parameters, a = 5.40 Å, b = 11.70 Å, c = 5.24 Å, and β = 91°. Intensity notations s, m, and w indicate strong, medium, and weak, respectively.
[b] Lattice spacings observed for sample 12b.
[c] Lattice spacings observed for sample 14.

DISCUSSION

From the results of group 1 catalysts with an atomic ratio of Bi/Mo = 2:3, we can conclude that the addition of a small amount of iron (sample 1) results in a mixture of the α-phase of bismuth molybdate, compound X, and ferric molybdate. With increasing iron content, the α-phase of bismuth molybdate is replaced by compound X if the calcination temperature is 500°C or greater and by a poorly crystallized compound if the calcination temperature is 450°C. Further increase in the amount of Fe results in a massive segregation of α-Fe_2O_3 which is especially evident in catalysts with large iron content. In addition, these results lead to the conclusion that the addition of Fe to catalysts with an atomic ratio of Bi/Mo = 2:3 results, at calcination temperatures of 550 and 600°C, in the formation of $Fe_2(MoO_4)_3$ which was observed in each case.

We can conclude from the results obtained for the group 2 catalysts that when the atomic ratio of [Bi + Fe]/Mo = 2:3 the formation of both the α-phase of bismuth molybdate and ferric molybdate is favored. This conclusion is especially evident in catalysts 10a and 10b of group 2 and is consistent with the information concerning the structure of these two molybdates. Ferric molybdate (*8*) is characteristic of molybdates having a $Sc_2(MoO_4)_3$ structure which is found for the class of compounds $A_2(MoO_4)_3$ where A is Al, In, Cr, Fe, or a small radius rare earth cation (*15*). The α-phase of bismuth molybdate (*16*), on the other hand, belongs to a class of molybdates having a structure similar to $Eu_2(WO_4)_3$ and $La_2(MoO_4)_3$ which are derived from the $CaWO_4$ (scheelite) structure (*17*). These molybdates characteristically contain cations with larger radii than those of the ferric molybdate class. Although both types of structure are monoclinic, the fact that they belong to different space groups and have different lattice parameters leads to the conclusion that they only will form a solid solution with difficulty. This conclusion is also consistent with the investigation of Batist *et al.* (*3*) involving preparations with the atomic ratio Bi + Fe/Mo = 2:3 for which the characteristic reflections of both $Bi_2(MoO_4)_3$ and $Fe_2(MoO_4)_3$ were observed. However, in contrast to the results of the investigation by Batist *et al.*, we do not observe the characteristic intensities of Bi_2MoO_6 in any of our catalysts.

When the molybdenum content is decreased, as in the group 2 catalysts, ferric molybdate systematically decreases, the α-phase of bismuth molybdate decreases, subsequently not detectable, and compound X predominates as is exemplified in the sample 12b. The deviation in the atomic ratio, as determined by elemental analysis, of sample 12 from Bi/Fe/Mo = 1:1:1 is reflected in the presence of $Fe_2(MoO_4)_3$ as a trace impurity. These results present evidence that compound X has an atomic ratio Bi/Fe/Mo = 1:1:1 and that an appreciable amount of iron exists in solid solution with compound X.

The results of the X-ray study yield conclusions regarding the formation and stability of the poorly crystallized compound and compound X. The poorly crystallized compound is formed at 450°C but is not stable when the calcination temperature is 550°C or higher. At calcination temperatures between 550 and 700°C, compound X is formed instead and appears to be stable.

The poorly crystallized compound, as seen in Table 3, is detected only in catalysts calcined at 450°C. In Table 4 we have compared the observed lattice spacings d_{hkl} for the poorly crystallized compound with the calculated lattice spacings for a tetragonal lattice of space group C_{4H}^6–$I_{41/A}$, using the parameters $a = 5.26$ Å and $c = 11.70$ Å. On the basis of the close agreement between the observed lattice spacings and the lattice spacings calculated for the scheelite unit cell, we conclude that the poorly crystallized compound has a scheelite structure.

Scheelite structures (*18*) have the ideal formula AMO_4 and exist for many molybdates and tungstates of divalent cations, e.g., $CdMoO_4$, $CaWO_4$, $PbMoO_4$, and $BaMoO_4$. Substitution of the divalent cation is possible giving scheelite compounds of the type $A^{+1}_{0.5}A^{+3}_{0.5}MO_4$, e.g., $Na_{0.5}Bi_{0.5}MoO_4$. Defects have been introduced according to the formula $Li_{0.5-3x}Bi_{0.5+x}\square_{2x}MoO_4$, where $\square$ represents a vacant lattice site which would normally be occupied by a divalent cation (*19*). Substitution of the divalent cation by trivalent ions such as Eu, La, and Bi results in structures which are derived from the $CaWO_4$ (scheelite) structure and can be represented by the formulas $Eu_{2/3}\square_{1/3}WO_4$, $La_{2/3}\square_{1/3}MoO_4$ and $Bi_{2/3}\square_{1/3}MoO_4$, respectively (*17*). The or-

dered arrangement of the vacancies gives rise to superstructures, e.g., $Bi_{2/3}\square_{1/3}MoO_4$ (the α-phase of bismuth molybdate) with ordered vacancies has a monoclinic structure with space group $P_{21/c}$ and unit cell parameters of $a = 7.685$ Å, $b = 11.49$ Å, $c = 11.929$ Å, and $\beta = 115°40'$ (*16,20*).

The X-ray data as a function of composition has recently been reported for bismuth molybdovanadates $Bi_{1-x/3}Mo_x$, $V_{1-x}O_4$ and for lithium bismuth molybdates $Li_{0.5-3x}Bi_{0.5+x}\square_{2x}MoO_4$ with scheelite structures (*21,19*). In Fig. 7, we have

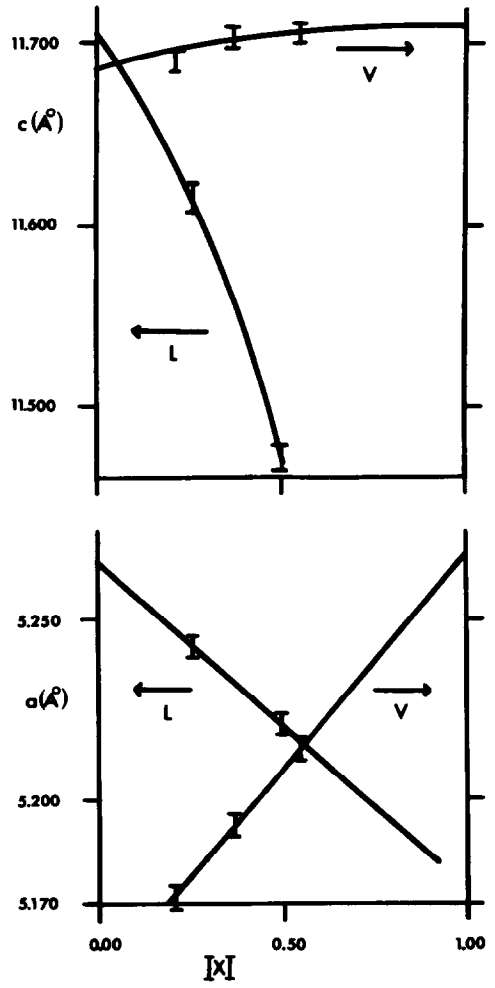

FIG. 7. Extrapolation of lattice parameters: (L) extrapolation to $Li = [X] = 0$ in the formula $Li_{0.5-3x}Bi_{0.5+x}\square_{2x}MoO_4$; (V) extrapolation to $x = [X] = 1$ in the formula $Bi_{1-x/3}Mo_xV_{1-x}O_4$.

extrapolated these results to $x = 1$ and $x = 0.5/3$, respectively, i.e., to $Bi_2(MoO_4)_3$, and obtain $a = 5.26$ Å and $c = 11.70$ Å which agree with the parameters calculated for the poorly crystallized compound.

The agreement of the parameters suggests a relationship between the poorly crystallized compound and a scheelite $Bi_{2/3}\square_{1/3}MoO_4$ structure. Although the structure of the α-phase of bismuth molybdate, $Bi_2\square_1(MoO_4)_3$, is derived from the scheelite structure, the ordered arrangement of vacancies gives rise to a monoclinic structure as discussed above. We consider that the broadness of the bands observed in the X-ray pattern of the poorly crystallized compounds possibly indicates the presence of a random distribution of vacancies and that the scheelite $Bi_{2/3}\square_{1/3}MoO_4$ structure of the poorly crystallized compound is stabilized by the random distribution of vacancies. The presence of iron apparently favors the formation of this scheelite $Bi_{2/3}\square_{1/3}MoO_4$ structure although Mekhtiev *et al.* (*22*) have reported that the α-phase of bismuth molybdate possesses a scheelite-type structure with a random distribution of vacancies.

An alternative and seemingly more possible explanation for the scheelite structure of the poorly crystallized compound is based on the elemental analysis and the close structural relationship between the poorly crystallized compound and compound X. We consider that the poorly crystallized compound is possibly a low temperature modification of the compound X structure and that the broadness of the bands results from a lack of complete formation of this compound at the 450°C calcination temperature, i.e., the poorly crystallized compound is completely formed at temperatures slightly higher than 450°C.

With an increase in the calcination temperature to 550 or 600°C, the X-ray data indicate that the low temperature poorly crystallized compound has transformed

into a compound very similar to compound X reported by Batist *et al.* (*3*). In addition, we observe splitting of several of the reflection lines which correspond to the poorly crystallized compound. The principles of X-ray crystallography predict that when the scheelite-type structure with a tetragonal lattice transforms into a monoclinic lattice, several X-ray reflection lines of the tetragonal lattice split into two or more reflection lines for the monoclinic lattice; the line with $hkl = 101$ splits into lines 110 and 011, the line 112 splits into $\bar{1}21$ and 121, the 200 line splits into 200 and 002, etc. Such splitting was observed when $BiVO_4$ having a scheelite-type structure with tetragonal lattice transformed into a monoclinic lattice which is related to the scheelite structure (*13*).

It therefore appeared that compound X, formed at higher calcination temperatures, could be described by a monoclinic unit cell derived from and strongly related to a scheelite unit cell. The best agreement between the lattice spacings d_{hkl} observed for compound X and calculated lattice spacings d_{hkl} was obtained by assuming a monoclinic unit cell with space group $I_{2/A}$ and parameters $a = 5.40$ Å, $b = 11.70$ Å, $c = 5.24$ Å, and $\beta = 91°$ (Table 5). The strong relationship of the compound X structure with scheelite structure is reflected in the closeness of its parameters to the cell parameters for the tetragonal scheelite structure, $a = b = 5.26$ Å, $c = 11.70$ Å, $\alpha = \gamma = \beta = 90$.

As indicated earlier, the α-phase of bismuth molybdate is replaced by compound X when the amount of iron is increased while maintaining a constant atomic ratio Bi/Mo = 2:3 and when the amount of molybdenum is decreased while maintaining a constant Bi/Fe ratio. Elemental analysis also has indicated that an appreciable amount of iron exists in compound X. The ordered arrangement of vacancies in the structure of the α-phase of bismuth molybdate, based on a scheelite structure,

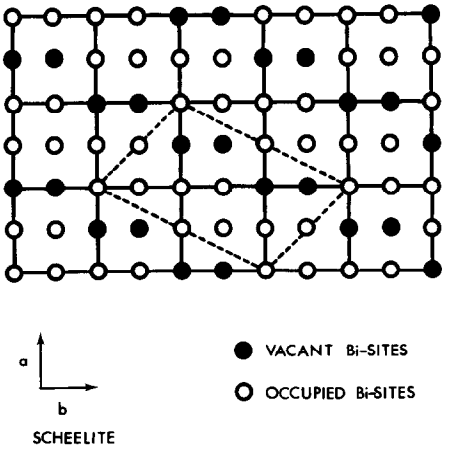

FIG. 8. Projection along the *c*-axis of Bi-sites in the scheelite structure (*16*): (—) unit cell of scheelite structure; (---) unit cell of monoclinic structure of $Bi_2(MoO_4)_3$.

results in a superstructure (monoclinic unit cell as shown in Fig. 8). We suggest that the presence of iron causes a filling of the vacancies in the α-phase of the bismuth molybdate structure, and this results in the stabilization of a structure more closely related to a scheelite structure, i.e., compound X (Fig. 9). We therefore propose when the atomic ratio Bi/Fe/Mo = 1:1:1, as in the case of compound X, that one Mo^{6+} ion is replaced by two Fe^{3+} ions: one Fe^{3+} ion (ionic radius = 0.64 Å) replaces one Mo^{6+} ion (ionic radius = 0.62 Å); the other Fe^{3+} ion occupies one of the vacancies. The replacement of Fe^{3+} by Mo^{6+},

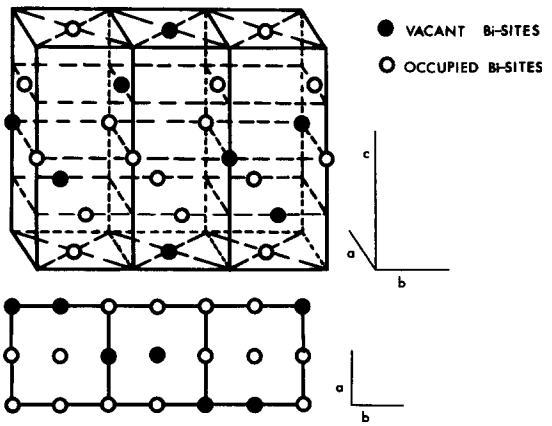

FIG. 9. Bismuth sites in scheelite structure.

a similar type of substitution, has been reported by Fagherazzi and Pernicone (*8*) for the formation of a Fe-defective ferric molybdate. Substitution is known to occur in the scheelite structure $Na_5Bi(MoO_4)_4$, i.e., Mo is replaced by Na, with a lower valence state than Mo (*23*). Moreover, Fe^{3+} can coexist with higher valence state ions as Nb^{5+} in compounds like $Pb[Fe_{1/2}Nb_{1/2}]O_3$, which forms a solid solution with $BeTiO_3$ (*24*). The proposed substitution can, therefore, be represented as $Bi_2Fe_{x/2}\square_{1-x/2}(Mo_{1-x/6}Fe_{x/6}O_4)_3$ in which $0 < x \leq 2$. When $x = 0$, the formula reduces to $Bi_2\square_1(MoO_4)_3$ which is the α-phase of bismuth molybdate. When $x = 2$, all of the vacancies are filled yielding the formula for compound X as $Bi_2Fe_2Mo_2O_{12}$. This formula indicates that for compound X the atomic ratio is Bi/Fe/Mo = 1:1:1 or Bi + Fe/Mo = 2:1.

Based on the previous discussion, we considered the possibility that similar types of substitutions occur in the Bi–Fe–Mo system and prepared catalyst 14, having the atomic ratio Bi/Fe/Mo = 3:1:2. As indicated earlier, the X-ray results showed a structure very similar to that of compound X (see Table 5). The deviation in the atomic ratio, as determined by elemental analysis of sample 14 from Bi/Fe/Mo = 3:1:2, is reflected in the presence of $Fe_2(MoO_4)_3$ as a trace impurity. These results present evidence that this compound has an atomic ratio Bi/Fe/Mo = 3:1:2 and a structure similar to that of compound X.

To account for the structure and composition of this compound, we propose a similar type of substitution: one Fe^{3+} ion replaces one Mo^{6+} ion, and one Bi^{3+} occupies one of the cation vacancy positions in the α-phase of bismuth molybdate structure. The proposed substitution yields a formula for this compound as $Bi_3FeMo_2O_{12}$. The slight deviation from a tetragonal unit cell for both compounds can be explained by the fact that although the ionic radii of Mo^{6+} and Fe^{3+} are approximately the same, the different polarization effects of these two ions cause a slight adjustment in the position of the atoms. This adjustment, therefore, results in a monoclinic unit cell which is essentially a distorted scheelite unit cell. Moreover, the X-ray pattern we observed is in excellent agreement with that reported by Sleight and Jeitschko (*25*) for a compound also having the atomic ratio Bi/Fe/Mo = 3:1:2. They too were able to satisfactorily index their X-ray data for this compound according to a monoclinic unit cell derived from a scheelite structure where there are trivalent cations in the tetrahdral sites. We, therefore, conclude that the compound we have prepared is identical to the compound prepared by Sleight and Jeitschko and that at least two pure ternary compounds (Bi/Fe/Mo = 1:1:1 and Bi/Fe/Mo = 3:1:2) can indeed form in the bismuth–iron–molybdenum system.

SUMMARY

In summary, our investigations indicate that addition of a limited number of Fe^{3+} ions to bismuth molybdate results in the stabilization of scheelite-type structures and the formation of ternary compounds. The scheelite-type structures can be explained by the filling of the cation vacancies in the α-phase of bismuth molybdate structure and undergo structural modifications with a variation in the calcination temperature. The Bi^{3+} ions and Fe^{3+} ions are apparently able to replace each other within these compounds with little structural change. We consider these compounds of interest both from a structural viewpoint and from a catalytic viewpoint. The results of an investigation of the physicochemical properties of these compounds have been reported earlier (*26*).

ACKNOWLEDGMENTS

The authors gratefully acknowledge partial financial support for this research from the Petroleum

Research Fund, administered by the American Chemical Society.

REFERENCES

1. Daniel, C., and Keulks, G. W., *J. Catal.* **29,** 475 (1973).
2. Annenkova, I. B., Alkhazov, T. G., and Belen'kii, M. S., *Kinet. Katal.* **10,** 1305 (1969).
3. Batist, P. A., Van de Moesdijk, C. G. M., Matsuura, I., and Schuit, G. C. A., *J. Catal.* **20,** 40 (1971).
4. McClellan, W. R., *U. S. Pat.* 3,415,886, 1968.
5. Keulks, G. W., Hall, J. L., Daniel, C., and Suzuki, K., *J. Catal.* **34,** 79 (1974).
6. Batist, P. A., Der Kinderen, A. H. W. M., Leewenburg, Y., Metz, F. A. M. G., and Schuit, G. C. A., *J. Catal.* **12,** 45 (1968).
7. Aykan, K., *J. Catal.* **12,** 281 (1968).
8. Fagherazzi, G., and Pernicone, N., *J. Catal.* **16,** 321 (1970).
9. Aravindakshan, N. I., and Ali, C., A. S. T. M. Powder Diffraction File: Scientific and Industrial Research (India), in press.
10. Zaslavskii, T. V., and Tutov, V. A., *Proc. Acad. Sci., USSR.* **5,** 1257 (1961).
11. Batist, P. A., Bouwens, J. F. H., and Schuit, G. C. A., *J. Catal.* **25,** 1 (1972).
12. Trifiro, F., Hoser, H., and Scarle, R. D., *J. Catal.* **25,** 12 (1972).
13. *Nat. Bur. Stand. (U.S.) Monogr.* 25 Sect. 3 (1963).
14. Kihlborg, L., *Acta Chem. Scand.* **13,** 954 (1959).
15. Abrahams, S. C., and Bernstein, J. L., *J. Chem. Phys.* **45,** 2745 (1966).
16. Van den Elzen, A. F., and Rieck, G. D., *Acta Crystallogr. Sect. B* **29,** 2433 (1973).
17. Jeitschko, W., *Acta Crystallogr. Sect. B* **29,** 2074 (1973).
18. Wyckoff, R. W. G., "Crystal Structures," 2nd ed., Vol. 3, p. 19. Wiley, New York, 1960.
19. Aykan, K., Sleight, A. W., and Rogers, D. B., *J. Catal.* **29,** 185 (1973).
20. Chen, T., *J. Cryst. Growth* **20,** 29 (1973).
21. Cesari, M., Perego, G., Zaggetta, A., Manara, G., and Notari, B., *J. Inorg. Nucl. Chem.* **33,** 3595 (1971).
22. Mekhtiev, K. M., Gamidov, R. S., Mamedov, K. S., and Bolov, N. V., *Dokl. Akad, Nauk. USSR* **162,** 563 (1965).
23. Wilson, A. J. C., "Structure Reports," Vol. 9, p. 173. Oosthoek, Utrecht, Netherlands, 1955.
24. Didkovskaya, O. S., Kovalevskaya, I. P., Seryi, V. G., Klimov, V. V., and Venevtsev, Y. N., *Sov. Phys. Crystallogr.* **18,** 184 (1973).
25. Sleight, A. W., and Jeitschko, W., *Mater. Res. Bull.* **9,** 951 (1974).
26. Notermann, T., Keulks, G. W., Skliarov, A., Maximov, Yu., Margolis, L. Yu., and Krylov, O. V., *J. Catal.* **39,** 286 (1975).